

## Nonlinear DC-response in Composites: a Percolative Study

Abhijit Kar Gupta and Asok K. Sen<sup>y</sup>  
 LTP Division, Saha Institute of Nuclear Physics  
 1/AF, Bidhannagar, Calcutta 700 064, India  
 (April 15, 2024)

The DC-response, namely the I-V and G-V characteristics, of a variety of composite materials are in general found to be nonlinear. We attempt to understand the generic nature of the response characteristics and study the peculiarities associated with them. Our approach is based on a simple and minimal model bond percolative network. We do simulate the resistor network with appropriate linear and nonlinear bonds and obtain macroscopic nonlinear response characteristics. We discuss the associated physics. An effective medium approximation (EMA) of the corresponding resistor network is also given.

PACS numbers: 64.60.Fr, 64.60.-i, 05.70.Fh

## I. INTRODUCTION

Formeasuring the susceptibility of a physical system, one generally studies its linear response for a small external perturbation such that this perturbation does not appreciably change the basic nature of the system governing the response characteristics under study. For an appropriately large perturbation (and a nondestructive one) the physical system may acquire newer modes of response and hence the system's response characteristic may change with the externally applied field.

Composite systems, which are the object of our study here, may be thought to be comprised of many microscopic elements or grains (much larger than atomic dimensions) having different physical properties. In the electrical case, it means that some of them may be metallic, some insulating and yet some others semiconducting. Further, the interface between them may also have different characteristics. If one takes the charge carrier (electron or hole) as a random walker, a metal corresponds to diffusive motion giving rise to Ohm's law. This diffusive behavior changes in the presence of tunneling across a barrier, like M-I-M, S-M-S, M-S-M, S-I etc. junctions (M stands for a metal, S a superconductor, and s a semiconductor). For example, a potential barrier called Schottky barrier arises within a semiconductor in intimate contact with a metal and gives rise to current  $i \propto \exp(-v/E_0)$ , where  $E_0$  is function of temperature. In

the case of a p-n junction heavily doped with Sb donors, the current seems to go from one linear region to another in steps, or the conductance smoothly connects two plateaus. Qualitatively similar curves [1] are observed for InP tunnel diode, Au doped Ge tunnel diode, etc. Further there could be inelastic processes by which an electron loses energy to the vibrational modes of species within the barrier. These processes thus provide extra paths or channels for current flow (thus increasing the conductance), and hence one may observe breaks in i-v curves joining two piece-wise linear (ohmic) regions. In the following percolative approach to obtain the direct current (DC) response of composite systems, one treats these elements semi-classically in the sense that one does not solve for the wave-function but takes the quantum mechanical effects indirectly by including only the tunneling currents through barriers [2].

It is clear that if these microscopic tunneling (nonlinear) elements become linear as discussed above beyond some characteristic microscopic voltage, then the nonlinear conductance of the whole system made up of such elements would change over to ohmic behavior (constant differential conductance) beyond some system-specific applied voltage. The point which may not be apparently obvious is that even if the nonlinear bonds remain so all the way upto infinity (i.e., their resistances become zero ('super'-conductor) at infinite voltage or frequency), the macroscopic system comprising of such bonds still saturates at high voltage to another linear region or ohmic behavior if the tunneling bonds do not percolate by themselves. In either case, the resistive behavior of the original percolative structure (zero voltage) guides the resistive behavior of the 'shorted' percolative structure. Thus, for vanishing driving fields, the system is in some state providing a fixed number of channels for the response, but asymptotically for infinitely large driving fields, the system is in another state representing a much higher number of channels. The generalized susceptibility (which could be thermal or electrical conductivity, any elastic modulus, or permeability, etc.) of this two (or, multi)-level system crosses over from one asymptotic linear region (value) to another (of higher saturation value) through some nonlinear region. It may be noted here that in rupture type of breakdown (e.g., electrical fuse [3]) phenomena, essentially the opposite thing happens, namely the system crosses over from a higher susceptibility value (highly efficient and stable network) to a lower one where the system cannot hold itself anymore. In electrical terminology, the system as a whole fuses to give rise to an

abhij@hp1.saha.emet.in  
<sup>y</sup>asok@hp2.saha.emet.in

insulator, or in mechanical terminology, the structure becomes mechanically unstable. Thus this enhancement or (de-enhancement) of the number of system-spanning channels and their eventual saturation as a function of some driving field is at the heart of the nonlinear response which is considered here in this work.

#### A. Experimental Facts

Nonlinear transport characteristics have been revealed in many different types of materials, including an early work by van Beek and van Pul (1964) on carbon-black loaded rubbers. References [4-7] in this regard are meant to be representative and not exhaustive. We discuss below some interesting and common features of composite materials, specially which are highly structured and give rise to some sort of universal behavior. Composite materials are typically a mixture of two or more phases, namely a mixture of metallic kind of material in an insulator where the mixture is not in the atomic scale. The metallic islands formed in the insulating matrix (as may be found by tunneling electron micrograph, TEM) are typically of dimensions much greater than the atomic size but much smaller than the macroscopic system size. As an example we may here refer to the carbon-black-polyvinylchloride (PVC) composites [8]. Carbon blacks composed of small but complicated shaped particles usually exist in the form of "high-structure" aggregates, whereas smaller and geometrically simpler particle aggregates are also possible and they are called "low-structure" blacks. A schematic description of such composites made of different forms or structures are given in Ref. [8]). The conductivity exponents for those three types of carbon-black-PVC samples were also measured. They were found to be  $t = 4$ ,  $t = 2.8$  and  $t = 2$  for "low-structure" (commercially called Mogul-L black), "intermediate-structure" (Cabot black) and "high-structure" composites respectively [8]. Only the "high-structure" composite ( $t = 2$ ) was found to be in the universality class of ordinary percolation problems and we actually have those kind of systems in our mind. In fact the following features pertain to a wide variety of such composite systems available.

**Very Low percolation threshold:** Usually these composites exhibit an unusually low percolation threshold. For example, in an experiment on carbon-wax system [5], there is a percolation transition at  $p_c = 0.0076$ . Very low thresholds are also reported for other systems, e.g.,  $p_c = 0.002$  for carbon-black-polymer composites [9] and  $p_c = 0.003$  for sulphonated (doped) polyaniline networks [10].

**Qualitatively identical I-V (as well as  $dI=dV$  vs.  $V$ ) response both below and above**

**threshold:** As an example one may note the experiment on Ag particles in KCl matrix by Chen and Johnson [7], where similar nonlinear transport was reported both below and above  $p_c = 0.213$ , even though the exponents for these two regions were reported to be grossly different. The fact that charge is carried even below  $p_c$  indicates that tunneling/ hopping between disconnected conducting regions does take place and is responsible for the nonlinearity.

**Power-law growth of conductance:** For small  $V$ , the excess conductance (above the constant/ohmic part) is claimed to grow as a non-integer power law with exponent  $\approx 1.36$  in 3D [5], whereas previous theoretical works took to be an integer equal to 2 to keep voltage inversion symmetry. Power-law in conductance against voltage ( $G-V$ ) automatically implies the power-law in  $I-V$  characteristics. The nonlinearity in  $I-V$  curves and the associated power-law have been observed in a variety of experiments (although in most of the experiments the  $G-V$  curves are not examined). Rimberg et al., [11] measured the  $I-V$  characteristics of one- and two-dimensional arrays of normal metal islands connected by small tunnel junctions and found a power-law:  $I \propto (V - V_g)^x$ ,  $V_g$  being the system's threshold voltage. The nonlinearity exponent is found to be  $1.36 \pm 0.16$  in the case of 1D array and  $1.80 \pm 0.16$  for 2D. However, the values of  $x$  were earlier predicted theoretically to be 1 and  $5/3$  in 1D and 2D respectively by Middleton et al. [12], through an approximate analytical calculation.

**Saturation of conductance:** In general for composite systems and for many other materials the  $G-V$  characteristics show a very interesting behavior. The  $G-V$  curve is seen to saturate for an appropriately high enough voltage below the Joule-heating regime. The typical curve then looks like a nonlinear sigmoidal type function interpolating two linear regimes. Some of the experiments [5,7] as mentioned above present the  $G-V$  data in this form for the purpose of proper analysis. A similar nonlinear curve for conductivity against field is also presented by Aertsens et al. [13] for microemulsions of water in oil under an external electric field.

**Crossover current for nonlinearity:** The current  $I_c$  (voltage  $V_c$ ) at which the conductance  $G$  differs from the zero-current (zero-voltage) conductance  $G_0$  by some small ( $\approx 1\%$ ) but arbitrarily chosen fraction is called the crossover current (voltage). It is seen to scale as  $I_c / G_0^x (V_c / G_0^{x-1})$ , where  $x$  is called the crossover exponent for nonlinearity. For carbon-wax composites,  $x = 1.4$  [5,6] in 3D, and for discontinuous thick gold films,  $x = 1.5$  as found by Gefen et al. [4]. One can easily

check that this exponent is related to above by  $\alpha = 1/(x - 1)$ .

Temperature-dependent conduction: Composite systems display very interesting temperature-dependent conduction properties particularly in the low temperature regime where the conduction is mainly due to phonon-assisted hopping of the electrons between randomly spaced localized states. One then needs to consider Mott's variable range hopping (VRH) or some of its variations namely  $\log G' \propto T^{-1/4}$  for low  $T$ . The conductance of the sample goes through a maximum as the temperature is increased still further towards some type of metallic behavior.

The first thing to note from the enlisted facts is the ultra-low percolation threshold even when the included conducting phases are isotropic. This along with the fact that many of these nonlinear systems carry current even below  $p_c$  indicates strongly that tunneling through disconnected (dispersed) metallic regions must give some virtually connected percolating clusters. From the nonlinear I-V characteristics (e.g., see the experiment by Chen and Johnson [7]) it is observed that the response behavior is reversible with respect to the applied field in the sense that the response curve (current or voltage) does almost trace back as the field is decreased. This fact also indicates that reversible tunneling is responsible for such a behavior. Also the temperature-dependent conductance with a maximum at some characteristic temperature (dependent on the amount of disorder present) and the Mott VRH type behavior at very low temperatures give further credence to tunneling assisted percolation. So, in the following section, we propose a semi-classical (or, semi-quantum) model of percolation [14] which works on the borderline between a classical and a quantum picture. Quantum physics enters our discussion through the possibility of tunneling of a charge carrier through a barrier (which does not exist classically).

One may consider a wide variety of nonlinear transport (apart from the nonlinear electrical conduction) processes and study them under the framework of percolation theory. One also exploits the key features and ideas of one such model and incorporate them into the other. As an example, one draws analogy between laminar flow in tubes and the electrical currents and uses the language of electrical network for convenience. The volumetric flow rate  $q$  is identified with the current  $i$  and the pressure drop  $P$  across a tube or a pore to the voltage difference  $v$  across a bond. Thus, for example, the flow of polymers is modelled (see e.g., Ref. [15] and references therein) considering a power law  $i = gv$  to each bond (tube or pore), where  $g$  is a generalized conductance. Considering the percolating network model of porous media one employs Monte-Carlo simulations or an effective medium approximation to calculate the rheological properties of a power-law fluid in flow through porous media. Foam

is a non-Newtonian fluid which is used in displacement and enhancement of oil recovery from the porous rocks. However, to move the foam through the pores, external pressure has to exceed a certain critical value  $P_c$ . In brittle fracture, no microcrack nucleation process takes place unless the applied stress exceeds a critical value for the system. A convenient description of this particular problem is done through the electrical analogue of breaking with the introduction of random fuse model [3]. One defines the 'fuse' as a device with a constant conductance when the applied voltage across it is less than a certain critical value  $v_c$ , beyond which it is an insulator. This electrical network model is a scalar analogue of the corresponding vector elasticity problem where the former is simpler to handle.

In most of the works we mentioned above, dilution plays an important role. These are models where the percolation theory has been the underlying framework and many of the interesting properties may be related to the cluster statistics. In this paper we first discuss briefly our proposed model for studying the effective nonlinear conduction properties of various composites. We then present the nonlinear current-voltage (I-V) characteristics in our model system and discuss the associated details.

## II. THE MODEL AND ITS PERCOLATIVE ASPECTS

To mimic charge transport in composite systems or dispersed metals, we assume the grains (metallic or metal-like) to be much larger than atoms but much smaller than laboratory-scale macroscopic objects. These grains are randomly placed in the host material which are insulators. Further we assume quantum mechanical tunneling between such grains across some potential barriers. Clearly these barriers would depend on the local geometry of the insulating and the metallic grains. Since in practice, the tunneling conductance should fall off exponentially, the tunneling should have some length scale designating an upper cut-off (for tunneling to occur) in the separation between two metallic grains. Further, the separation between two grains or the potential barrier can vary continuously between zero and some upper cut-off. For simplicity and to capture the basic physics, we construct a bond (lattice) percolation model for this problem, such that tunneling may take place only between two nearest neighbor ohmic conductors (or, o-bonds) and no further. Thus one may imagine a virtual bond sitting at each such gap which conducts current nonlinearly due to tunneling phenomenon. We call these tunneling conductors as tunneling bonds (or, t-bonds).

We stress again that our approach would be to solve an appropriate electrical network based on a semi-classical (or, semi-quantum) percolation model. Made of both random resistive and tunneling elements, this network

would be called a random resistor cum tunneling-bond network (RRTN) [16]. Now tunneling may take place through the tunneling bonds in various ways, so that the functional form of the tunneling current as a non-linear function of the potential difference across them may be quite complicated. For simplicity, we address the aspects of nonlinearity in a macroscopic system which comes through two piecewise linear regions of a t-bond such that the conductance is zero upto a threshold voltage and a given non-zero value beyond. In this context, it may be noted that disorder in many quantum systems like charge-density-wave (CDW) systems or flux-vortex lattices of type-II superconductors can give rise to 'pinning' or inhibition to transport upto a critical value of the applied field above which tunneling is active. The piecewise linear transport is in fact a highly nonlinear process as there is a cusp singularity at the intersection point. The transport due to tunneling which is the source of nonlinearity in the experimental systems [6,7] we focus on, can be well approximated in this way and thus the nonlinearity of the macroscopic system may be understood at a qualitative (and, sometimes even at a quantitative) level. Next, one notes as discussed above that in many physical systems, the response is negligibly low (or there is no response at all) until and unless the driving force exceeds a certain threshold value. A class of problems exist where sharp thresholds to transport occur. The examples in the electrical case are a Zener diode, a CDW system or a type-II superconductor and in the fluid permeability problems, for example, a Bingham fluid (where there is a critical shear stress  $\sigma_c$ , above which it has a finite viscosity and below which it is so enormously viscous that it does not flow). In our RRTN model, we work with t-bonds which have zero conductance below a threshold; see Fig. 1.

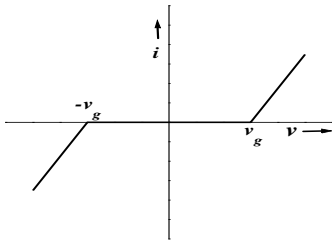


FIG. 1. The piecewise linear current-voltage ( $i$ - $v$ ) characteristic of each tunneling conductor.

Let us look at the uncorrelated random bond percolation first. In this model, the conducting o-bonds are occupied randomly with a certain volume fraction  $p$ . One uses a random number generator which generates random numbers distributed uniformly in the interval  $[0, 1]$ , to fix the positions of o-bonds in a certain configuration. So the system now has  $p$  fraction of occupied bonds and  $q = (1-p)$  fraction of unoccupied bonds. Up to this it is the standard (uncorrelated) bond percolation problem where

the percolation threshold in a square lattice is  $p_c = 0.5$ . A geometrical connection (or a system-spanning cluster of o-bonds) is established from one end of the bond configuration averaged system to the other only at or above this volume fraction in an infinite size system. If the occupied bonds are ohmic conductors and the unoccupied bonds correspond to insulators (the host) then we have the corresponding random resistor network (RRN) which carries an average non-zero current only when the volume fraction,  $p > p_c$ . Clearly this response is linear or ohmic.

But, our percolative model is not just a random mixture of two phases. For our convenience we take a square lattice in 2D. The basic physics should remain the same if we go over to 3D. As usual, the o-bonds are thrown at random at a certain volume fraction  $p$ . The rest  $(1-p)$  fraction contains insulators. Now we allow tunneling bonds (t-bonds) only across the nearest-neighbor (nn) gaps of two conducting bonds (and no further) if an appropriate voltage is applied externally across two opposite sides of the RRTN. The RRTN model is now comprised of ohmic conductors, pure insulators and some non-ohmic (tunneling) conductors. To have a clearer view of the proposed model system we refer to the Figs. 2 where we show all the ohmic bonds thrown at a concentration  $p$ , and all possible t-bonds. In the Fig. 2(a), we show a realization of a square lattice at  $p = 0.15$  in 2D where the system does not have any connectivity from one end to the other even if we consider all the t-bonds to be active. In the Fig. 2(b) at  $p = 0.25$ , there is a system spanning cluster (network) of o-bonds and t-bonds even though the system is actually below the geometrical threshold ( $p < p_c$ ). This demonstrates that the effective percolation threshold [17] of the system is lowered as the t-bonds come into play. Thus even if the system is below  $p_c$ , and hence has zero conductivity at a vanishingly small voltage, its conductivity will be non-zero and keep growing at appropriately higher voltages, and hence the system will behave non-ohmically. If the system is already above the geometrical threshold ( $p_c = 0.5$ ) then the t-bonds simply add extra paths to the already existing current carrying network (backbone) of o-bonds and give rise to similar non-ohmic behavior.

If we consider the percolative aspects of the model system at very large voltages (suppose all the t-bonds overcome their threshold and conduct ohmically), then this is no more a pure bond percolation problem of a random binary mixture. Rather we may think of it as a very specific correlated bond percolation problem. This is because the positions of the t-bonds are totally correlated to the positions of randomly thrown o-bonds. The disorder is in the position of the o-bonds only. Once the positions of the o-bonds are given for a particular configuration, the positions of the t-bonds are automatically determined for that configuration in our model. We have found out earlier [18] that the new percolation threshold with all the t-bonds added is  $p_{ct} = 0.181$ . We have also addressed [18] the question of universality class of this problem in this limit and found that the problem belongs to the same

universality class as that of the pure (uncorrelated) bond or site percolation.

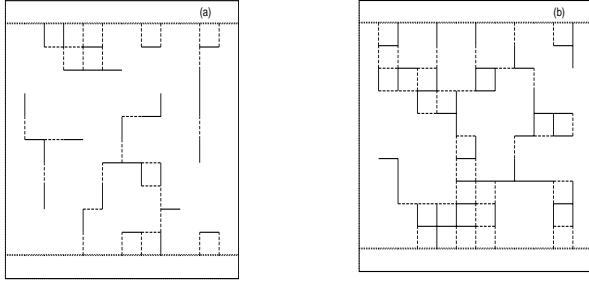


FIG. 2. Two typical configurations of a square lattice of size  $10 \times 10$  with  $p < p_c$  and an arbitrary but very large voltage where all the tunneling bonds indicated by broken lines are active. (a) For  $p = 0.15$  the system is seen to have no connecting path across its two ends even when one considers the tunneling bonds. (b) This configuration at  $p = 0.25$  is seen to have no connecting path with only ohmic bonds, but has at least one such path comprised of both the ohmic and the tunneling bonds.

### III. EFFECTIVE MEDIUM APPROXIMATION (EMA) FOR THE CORRELATED BOND PERCOLATION MODEL

An effective medium approximation gives reasonable result for any  $p$  away from the threshold (here  $p_{ct}$ ). The EMA has been used to calculate fairly accurate conductivity behavior for general binary mixtures except in the vicinity of the critical regions. This approach is old and had been devised for the transport properties of inhomogeneous materials first by Bruggeman [19] and then independently by Landauer [20]. Its successful application to the percolation theory by Kirkpatrick [21] has drawn attention of many others in this field. It has then been applied for a wide variety of inhomogeneous materials. The development has some similarity with the well-known coherent potential approximation (CPA) for treating the electronic properties of the binary alloy problem. The composite systems have seen a series of attempts in this direction while dealing with the nonlinearity in the response involved (see Ref. [22] and references therein).

Here we follow the method as described in ref. [21]. The method is as follows. Consider a random electrical network on a hypercubic lattice of dimension  $d > 1$  ( $d = 2$  for 2D,  $d = 3$  for 3D etc.). The basic idea is to replace a random network by a homogeneous effective network or an effective medium where each bond has the same average or effective conductivity  $G_e$ . The value of the unknown  $G_e$  is calculated in a self-consistent manner. To accomplish this, one bond embedded in the effective medium is assigned the conductivity distribution of the actual random network. The value of  $G_e$  is then determined with the condition that the voltage fluctuation across the special bond within the effective medium,

when averaged over the proper conductivity distribution, is zero. The voltage ( $v$ ) developed across such a special bond can be calculated [21] for a discrete lattice of  $z$  ( $= 2d$  for a hypercubic lattice) nearest neighbors as

$$v / (G_e - g) = [g + (d-1)G_e] \quad (3.1)$$

The requirement is that the average of  $v$  be zero when the conductance for the special bond may take any of the ohmic, the tunneling or the insulating bond value with appropriate probabilities for the actual network.

The probability of a bond to be ohmic, tunneling or purely insulating according to the considerations of our model is given below for 2D square lattice.

$$P_o = p; \quad (3.2)$$

$$P_t = (p^3 + 3p^2q + 3pq^2)^2 q; \quad (3.3)$$

$$P_i = [1 - (p^3 + 3p^2q + 3pq^2)^2] q; \quad (3.4)$$

where  $q = 1 - p$ . For a distribution of three types of resistors, we have

$$f(g) = P_o(g - g_o) + P_t(g - g_t) + P_i(g - g_i); \quad (3.5)$$

where  $g_o$ ,  $g_t$  and  $g_i$  are the conductances of ohmic, tunneling and the insulating resistors respectively. The EMA condition stated above i.e.,  $\langle v \rangle = 0$  reads

$$\sum_z dgf(g) (G_e - g) = [g + (d-1)G_e] = 0; \quad (3.6)$$

Putting Eq. (3.5) into the above Eq. (3.6), we get

$$\frac{P_o(G_e - g_o)}{[g_o + (d-1)G_e]} + \frac{P_t(G_e - g_t)}{[g_t + (d-1)G_e]} + \frac{P_i(G_e - g_i)}{[g_i + (d-1)G_e]} = 0; \quad (3.7)$$

The above equation reduces to the quadratic equation

$$AG_e^2 + BG_e + C = 0; \quad (3.8)$$

where  $A = (d-1)^2$ ,  $B = [(d-1)(P_t + P_i)g_o + (d-1)(P_o + P_i)g_t - (d-1)^3(P_o g_o + P_t g_t)]$  and  $C = [P_i g_o g_t - (d-1)g_o g_t (P_o + P_t)]$ , considering the conductance of the insulating bonds to be  $g_i = 0$ . The valid solution of Eq. (3.8) is

$$G_e = \frac{B + (B^2 - 4AC)^{1/2}}{2A}; \quad (3.9)$$

Now one can obtain the linear conductance of the macroscopic model composite system in 2D and 3D, putting  $d=2$  and 3 respectively, given some specific values or functional forms for the conductances of the elementary components like the ohmic and the tunneling bonds.

In our model we have assumed that the conductance of a tunneling bond, when it overcomes its voltage threshold, is the same as that of an ohmic bond. We believe that this assumption does not change the phase transition characteristics. Now in the limit of large enough

external voltage if we assume  $g_t = g_o = 1$  and  $g_i = 0$ , we have

$$G_e = \frac{d(P_o + P_t)}{(d-1)}; \quad (3.10)$$

At the percolation threshold  $p_{ct}$  the effective conductance ( $G_e$ ) of the system is zero. In 2D we now have the following equation putting  $d = 2$  in Eq. (3.10),

$$2(P_o + P_t) = 1; \quad (3.11)$$

Solution of the above equation gives  $p = p_{ct} = 1/4$ . This may be compared with our simulation result [18] which gives  $p_{ct} = 0.181$ . The EMA is basically a mean field calculation which overestimates the percolation threshold value in lower dimensions. However, for pure bond percolation in 2D, this gives the exact result  $p_c = 1/2$ . This is so because the square lattice in 2D is self-dual in the case of purely random bond percolation problem.

We may also find the value of  $p_{ct}$  for 3D where the probability of tunneling bond is

$$P_t = (p^5 + 5p^4q + 10p^3q^2 + 10p^2q^3 + 5pq^4)^2q \quad (3.12)$$

Using  $d = 3$  in Eq. (3.10), an equation similar to Eq. (3.11) is obtained, which when solved gives  $p_{ct} = 1/8$  exactly.

#### IV. THE NONLINEAR I-V CHARACTERISTICS

For the work presented below, we make the simplifying assumption that all the tunneling bonds (t-bonds) in our RRTN model have an identical voltage threshold ( $V_g$ ) below which they are perfect insulators and above which they behave as the ohmic bonds. One could certainly introduce disorder by making  $V_g$  random as in Ref. [23]. In our case disorder is already introduced through random positioning of the bonds, and we believe that our assumption should not affect the dilution-induced nonlinearity exponents. Indeed, as shown in the sequel, our model gives richer possibilities (dilution dependence) for the nonlinearity exponent in a composite system.

As the externally applied field (DC) is increased beyond some macroscopic threshold, some of the t-bonds overcome their microscopic thresholds and may thus increase the overall conductance of the system if the process leads to newer parallel connectivities for the whole macroscopic composite. Our computer simulation to study these effects [24] involves the solution of Kirchhoff's law of current conservation at the nodes of the RRTN with the linear and the nonlinear (assumed piecewise linear) resistors and the standard Gauss-Seidel relaxation. Current response was averaged over 50 configurations in all the cases mentioned here. We obtain current ( $I$ ) against voltage  $V$  and therefrom the differential conductance ( $G = dI/dV$ ) for the whole network at

a given volume fraction  $p$  of the ohmic bonds. Simulation results for nonlinear I-V curves for a square lattice of size  $L = 40$  are plotted in Fig. 3 for  $p = 0.3$  to  $0.9$ . For  $p > p_c$ , one may note that the I-V curve is linear up to a certain voltage ( $V_g$ ), beyond which the nonlinearity shows up. For  $p < p_c$ , there is no current (zero conductance) below a threshold voltage ( $V_g$ ), beyond which the nonlinear conduction starts. Nonlinearity is always there in the I-V response for any value of  $p$  in the interval  $p_{ct} < p < 1$ . However, for  $p_{ct} < p < p_c$ , there is no system-spanning path with the ohmic bonds (in an average sense) and the response (average current) is zero for small voltages. The response in this case starts out nonlinearly from a non-zero average threshold voltage. On the other hand, for  $p > p_c$ , the system always has a conducting path through the ohmic bonds (again on an average), and so up to a certain voltage ( $V_g$ ) there is a constant non-zero conductance and the average response is linear. As  $V$  is increased beyond  $V_g$ , more and more current carrying paths are added with the help of the t-bonds and in effect the conductance starts increasing with  $V$ .

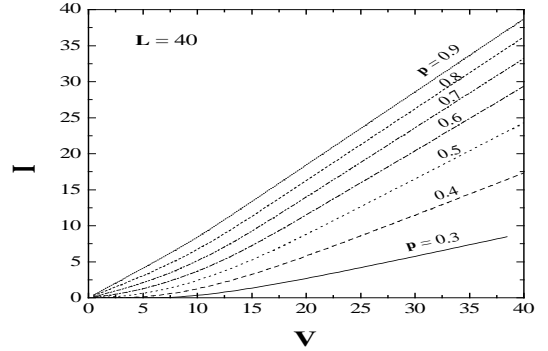


FIG. 3. A set of nonlinear I-V curves for  $p = 0.3$  to  $0.9$  for the RRTN network of size  $40 \times 40$ . The current response is averaged over 50 configurations each.

We find that the entire nonlinear regime of a I-V curve can not be fitted by a simple power-law which in general may be fitted by a polynomial function. Even after doing that, the exponent of nonlinearity from the fitting of the various I-V curves remained somewhat ambiguous since the fitting was not very robust. Thus to have a better idea, we obtain the differential conductance ( $G = dI/dV$ ) by taking the numerical derivative of the I-V data. In these derived  $G-V$  curves, one can identify the threshold voltage  $V_g$  as the onset of nonlinearity and the onset of the saturation regime ( $G_f$ ) much more clearly than in the I-V curves. The  $G-V$  curves corresponding to  $p = 0.7$  and  $0.3$  in the Figure 3 are shown in the Figs. 4 and 5 respectively. As expected for the two different cases, in Fig. 4 ( $p > p_c$ ) the initial conductance has a finite nonzero value ( $G_0 \neq 0$ ), while in the Fig. 5 ( $p < p_c$ )

the initial conductance is zero ( $G_0 = 0$ ). The general nature of the  $G$ - $V$  characteristics is that eventually all of them become saturated, i.e., assume a constant and  $p$ -dependent conductance beyond some very large voltage  $V_s$ . The reason is that for a finite-sized system there is always a very large but finite voltage  $V_s$  at which the conductance of the whole system saturates to an upper maximum value  $G_f$  (another linear regime) since all the possible  $t$ -bonds become activated and no more channel parallel to the backbone come into play for a further increment of  $V$ . Below we concentrate on the analysis of the nonlinear conductance behavior of the model system in an effort to first find a general functional form to describe all these different  $G$ - $V$  curves and then to find the exponent of nonlinearity at different volume fractions.

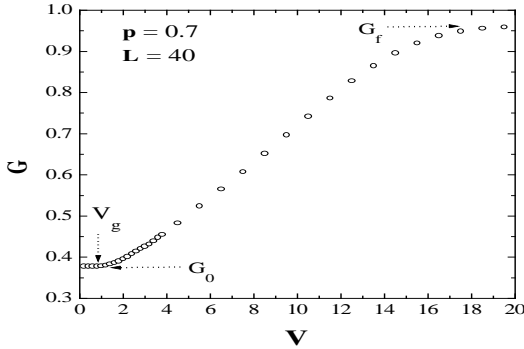


FIG. 4. The  $G$ - $V$  curve corresponding to  $p = 0.7$  of Fig. 3 ( $p > p_c$ ). The threshold voltage ( $V_g$ ) is indicated in the Figure. Initial conductance ( $G_0 \neq 0$ ) and the final conductance ( $G_f$ ) are also indicated.

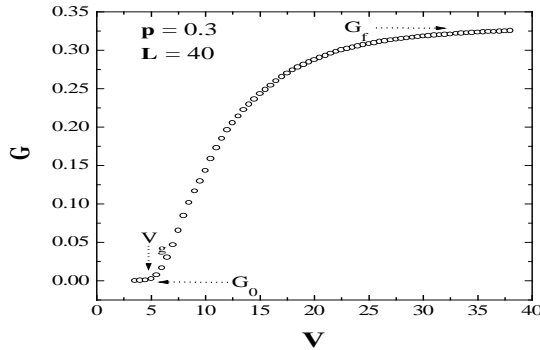


FIG. 5. The  $G$ - $V$  curve corresponding to  $p = 0.3$  of Fig. 3 ( $p < p_c$ ). The threshold voltage ( $V_g$ ) is indicated in the Figure. Initial conductance  $G_0 = 0$  and the final conductance ( $G_f$ ) is as indicated.

#### A. Analysis of the Behaviour of Conductance

Guided by the conductance behavior of a complex system made out of many simple prototype circuits [14] and by the fact that the initial power-law type growth of  $G$  beyond  $G_0$  finally saturates to  $G_f$ , we try to fit the whole region in our simulation by a function of the form:

$$G = G_0 \quad (V < V_g) \quad (4.1)$$

$$= G_f - G_d [1 + (V - V_g)^{-\alpha}] ; \quad (V > V_g); \quad (4.2)$$

where  $V = V - V_g$  is the shifted voltage from where nonlinearity appears. For concreteness, we discuss here the fitting of a sample data set for  $L = 40$ ,  $p = 0.6$ . For this sample  $G_0 = 0.154$ ,  $G_f = 0.881$ . The parameters for the best fit in this case as obtained by a simplex search procedure are  $\alpha = 3.27 \times 10^4$ ,  $\beta = 1.408$ , and  $\gamma = 125$ . Such large values of  $\alpha$  are obtained for all the cases studied and yet the approach to  $G_f$  was slower than in actual data. This obviously indicates that the approach to saturation is not a power-law type and probably an exponential function is involved. At this point we refer to the Fig. 6 where we have shown a  $G$ - $V$  curve for  $p = 0.8$  and  $L = 40$  for which the conductance ( $G$ ) seems to saturate (to the naked eye) at a voltage above  $V = 20$  and one can see a practically flat regime in between  $V = 20$  to  $40$ . However, in the same figure we have demonstrated in the inset by zooming in on the  $y$ -axis that the actual saturation is yet to come and that the conductance ( $G$ ) in this regime increases very slowly with  $V$ . The reason is that there are some tunneling bonds (typically in the transverse direction to the electric field) which do not become active even with the application of a very large voltage implying that the conductance for the whole system is yet to reach the complete saturation. This pathology supports the fact that the final saturation occurs at an extremely large voltage, and that the approach to the saturation is indeed very slow.

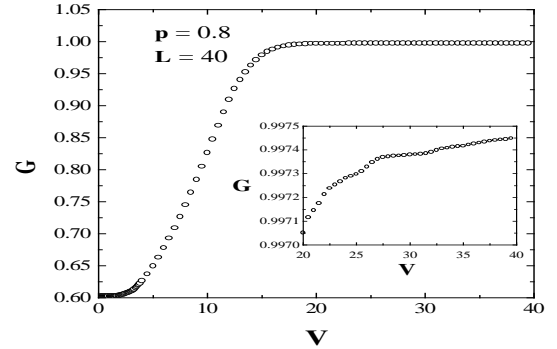


FIG. 6. A typical  $G$ - $V$  curve for  $L = 40$  and  $p = 0.8$  with an apparent onset of the saturation regime beyond  $V = 20$ . The inset shows that the  $G$  does not yet saturate in the true sense and instead ever increases in the regime  $20 < V < 40$ .

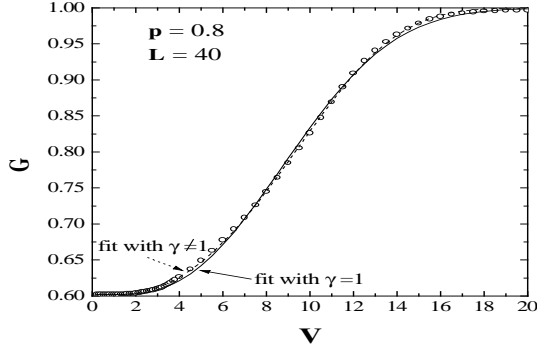


FIG. 7. The demonstration of the fitting of a  $G$ - $V$  curve by the proposed function (4.7) shown for  $L = 40$  and  $p = 0.8$ . The fitting is better with  $\gamma \neq 1$  (shown in dashed line) for the entire data set than that with  $\gamma = 1$  (shown in full line).

We tried the following four plausible functions involving exponentials for the entire nonlinear regime replacing the above Eq. (4.2).

$$G = G_0 + G_d \exp(\gamma V) \quad (4.3)$$

$$= G_0 + G_d \tanh(\gamma V) \quad (4.4)$$

$$= G_f - G_d \exp[\gamma \exp(V)] \quad (4.5)$$

$$= G_0 + G_d [1 - \exp(-\gamma V)] \quad (4.6)$$

Out of all the optimally fitted functions as described above, the last Eq. (4.6) is the best in the sense that it gives the minimum mean square deviations (MSD) for the  $G$ - $V$  data. It may be noted that a special case of Eq. (4.6) with  $\gamma = 1$  was the form of nonlinearity used by Chen and Johnson [7] in fitting their experimental conductance against voltage data for a composite system of Ag-KCl. But for all  $p$  and  $L$ 's considered by us,  $\gamma = 1$  was found inadequate for fitting the typical sigmoidal curves. For example we have shown in Fig. 7, the fitting with the function (4.6) for  $p = 0.8$ ,  $L = 40$ : the restricted case of  $\gamma = 1$  shown by full line, and an unrestricted, optimally fit  $\gamma \neq 1$  by dashed line. Clearly the unrestricted case fits the data extremely well and gives an MSD which is much smaller than that of the restricted case as mentioned above.

#### B. The Nonlinearity and the Crossover Exponent

The conductance ( $G$ ) for metal-insulator composite systems starts growing nonlinearly with the applied voltage  $V$  from an initial value ( $G_0$ ) and finally saturates to a value  $G_f$  (as indicated in the Figures 4 and 5).  $G_0$  is the conductance when none of the  $t$ -bonds is active; this happens in the usual percolation model, without tunneling. Likewise,  $G_f$  is the conductance when all the so-called tunneling bonds ( $t$ -bonds) are actually active and taking part in the conduction. There are three distinct regimes

which, in general, can be precisely located from the  $G$ - $V$  characteristics than from the  $I$ - $V$  characteristics:

- (i) Up to some voltage  $V_g$  the initial conductance ( $G_0$ ) of the system is either zero or a fixed finite value depending on whether the system has initially conducting path through the ohmic (or metallic) bonds or not (see Figs. 4 and 5).
- (ii) Beyond  $V_g$  the nonlinearity starts showing up. The conductance ( $G$ ) is nonlinear in the regime  $V_g < V < V_s$ .
- (iii) Beyond the voltage  $V_s$ ,  $G$  saturates to a voltage  $G_f$  (see Figs. 4 and 5).

The data obtained through our model system in 2D were fitted through the following general formula as discussed above:

$$G = G_0 + G_d [1 - \exp(-\gamma V)] ; \quad (4.7)$$

where  $G_d = G_f - G_0$ . Clearly, irrespective of the value of  $V_g$ ,  $G_0$  is the conductance in the limit  $V \rightarrow 0$ . Experimentally  $G_f$  may be obtained by applying a large enough voltage such that Joule heating remains unimportant. In our computer simulation on finite sized systems, we find  $V_s$  to be a large but finite voltage (in arbitrary units). For example for squares with  $L=40$ ,  $V_s$  is found to be typically of the order of  $10^4$ - $10^6$ .

In a recent experiment by Chen and Johnson [7] in Ag-KCl composite (silver particles in KCl matrix), very similar  $G$ - $V$  curves were obtained and the non-ohmic effect was postulated to arise from a localized reversible dielectric breakdown between narrowly separated metal clusters in the metal-insulator composite. The intercluster or interparticle spacing may have some distribution which is related to the fractal dimension  $d_f$  of the network at the threshold. Chen and Johnson [7] used the following conductance behavior for their data:

$$G = G_0 + (G_f - G_0) [1 - \exp(-V/V_g)^{n(d_f)}] ; \quad (4.8)$$

which is a special form of the function (4.7) we propose. We find Eq. (4.8) to be inadequate for the representation of our and experimental data (see above). The exponent  $n(d_f)$  is in fact the same as  $\gamma$  and is hence related to the nonlinearity exponent (see Sec. IA) by  $\gamma = n(d_f) + 1$ . It has been further shown in the above work that  $n(d_f)$  increases as the silver volume fraction is decreased and it shows a sharp change at the threshold. We shall discuss in this section how our model captures this dilution-dependent nonlinearity exponent.

For a meaningful comparison of all the  $G$ - $V$  data with different  $G_0$ ,  $G_f$ ,  $V_g$ , etc., we look at the scaled conductance  $\bar{G} = (G - G_0)/G_d$  against the scaled voltage  $\bar{V} = (V - V_g)/V_g$ . To see if the  $G$ - $V$  data for various values of  $p$  both below and above  $p_c$  scale, we first looked within the range  $0.48 < p < 0.52$  (i.e., very close to  $p_c$ ),



and found that all the data do reasonably collapse. In the Fig. 8 we show such a plot for a 20 × 20 system. This suggests the following general form for the functional behavior;

$$G = f(\tilde{V}); \quad (4.9)$$

where  $f(x)$  is a function such that  $f(0) = 0$ , and  $f(1) = 1$  and is otherwise quite general as long as it represents the behavior of  $G$  very well. Clearly the scaled function in Eq. (4.7) satisfy these properties very well.

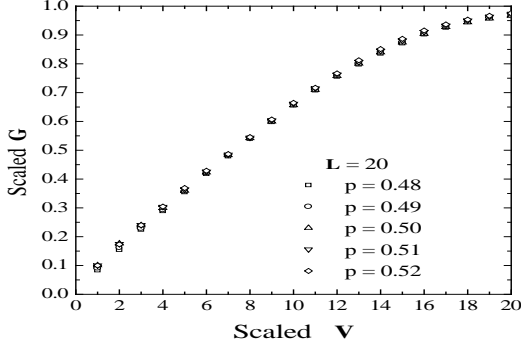


FIG. 8. The plot of scaled conductance against scaled voltage for various  $p$  around  $p_c$ .

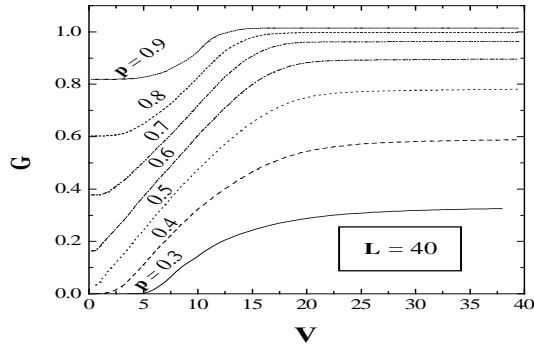


FIG. 9. The family of  $G$ - $V$  curves corresponding to the Fig. 3.

Here we point out that the threshold voltage  $V_g$  is the only relevant variable that enters into the scaling function. The other voltage scale  $V_s$  which is the onset voltage for saturation, is seen to have no role in the above scaling Eq. (4.9). For small  $V = V - V_g$ , i.e., near the onset of nonlinearity, the excess conductance  $G = G - G_0$  varies with the voltage difference ( $V$ ) as a power-law as one may easily check by expanding Eq. (4.7) in the limit ( $V \rightarrow 0$ ):

$$G - G_0 \propto V^\beta \quad (4.10)$$

Thus the nonlinearity exponent is related to the fitting parameters  $\beta$  and  $\gamma$  by  $\beta = \gamma / (\gamma - 1)$ . In our earlier work [14] with our preliminary observations we had reported the nonlinearity exponent to be close to 1 and to be independent of  $p$  near the geometrical percolation point  $p_c = 0.5$ . Indeed, in most of the experiments an average value of the above exponent is reported for the data for samples close to  $p_c$ .

Further careful analysis of the results at widely different volume fractions indicate that the nonlinearity exponent increases significantly as we go sufficiently away from the percolation threshold (both below and above). This becomes apparent from the shape of the  $G$ - $V$  curves for different volume fractions in a wide range of  $p$  (from 0.3 to 0.9) in Fig. 9 corresponding to the  $I$ - $V$  curves shown in Fig. 3. In Fig. 10 we plot the scaled conductance ( $G$ ) against scaled voltage ( $\tilde{V}$ ) corresponding to all the  $G$ - $V$  curves in Fig. 9. The scaled data for all the curves now do not fall on top of each other indicating that all of them can not be described by the same fitting parameters  $\beta$  and  $\gamma$ , even though the form of the best

fitting function  $f(x)$  remains the same. Hence the nonlinearity exponent in the power-law regime ( $V \rightarrow 0^+$ ) for these curves of different  $p$  are not identical.

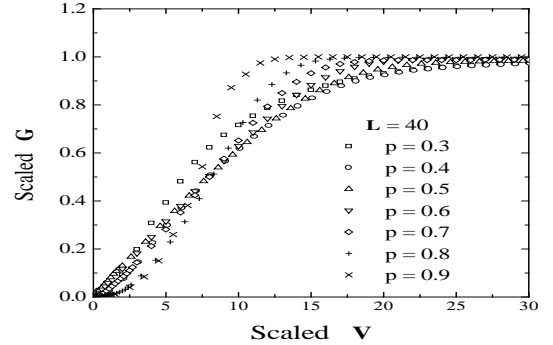


FIG. 10. The scaled conductance against the scaled voltage for different  $p$  (both below and above  $p_c$ ) corresponding to the curves in Fig. 9. The data do not collapse at all indicating different exponents for different  $p$ 's.

The fitting of the individual  $G$ - $V$  curves for squares of sizes  $L = 20$  and  $40$  and some data for  $L = 60$  and  $80$  for different  $p$  in the range of  $p = 0.2$  to  $0.9$  were done by using Eq. (4.7). The Fig. 11 demonstrates that the exponent  $\beta$  for  $L = 40$  increases from a value close to 1 at  $p = p_c$  to values close to 3 and above on either side ( $0.3 \leq p \leq 0.9$ ). We found that the value of  $\beta$  at  $p_c$  lies in the range 0.97 to 1.04 for system sizes  $L = 10$  to  $60$ . There is no systematic variation with  $L$  and this indicates the absence of any finite size dependence for the above exponent at  $p_c$ . Thus within our numerical accuracy we find that  $\beta(p_c) = 1.0$ . It is thus clear from the Fig. 11 that  $\beta(p_c)$  is the minimum of the  $p$ -dependent exponent

(p). Note that the nonlinearity exponent for the I-V curves would be just  $\beta = \alpha + 1 = 2.0$  (in this case), where  $I \propto (V - V_g)^\alpha$ , and for  $p$  sufficiently far from  $p_c$ , would also show the same concentration dependence. In comparison, we observe that in an experiment on 2D arrays of normal metal islands connected by small tunnel junctions, Rinberg et al. [11] found the nonlinearity exponent to be  $1.80 \pm 0.16$ . It may also be noted that Roux and Hermann [23] also obtained from their simulation of the I-V nonlinearity exponent  $\beta = 2$  in their model 2D network with the resistors without any dilution but with random thresholds. Clearly thus, our bond-diluted RRTN model is richer than the random threshold model at least as far as the nonlinearity exponent is concerned.

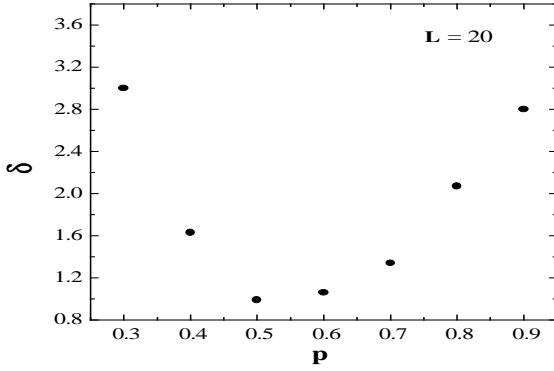


FIG. 11. The variation of nonlinearity exponent ( $\beta$ ) for the  $I$ - $V$  curves with  $p$  for a system of size  $40 \times 40$ .

Now we discuss the crossover exponent which is an alternative way of accounting for the strength of nonlinearity. The crossover exponent ( $x$ ) is defined from the power-law relationship  $I_c \propto G_0^x$  where  $I_c$  is the crossover current at which the conductance of the system has increased from a nonzero initial value  $G_0$  by a small but arbitrarily fixed fraction  $\epsilon$ . So  $x$  is defined only above  $p_c$ . The value of the above exponent was calculated by Gefen et al., [4] from the experimental nonlinear response data of discontinuous thick gold films near and above the percolation threshold (in 3D). Their experimental measurement gives  $x = 1.47 \pm 0.10$ , whereas they argue through a model resistor network [16] that the value of  $x$  should be  $3/2$  (in 3D). The argument is based on the assumption of a power law dependence of conductance ( $G$ ) which interpolates between its initial value  $G_0$  (at  $V = V_g$ ) and the saturation value  $G_f$  ( $V = V_s$ ). Note that the crossover exponent for the carbon-wax experiment in 3D is also close to this value. Gefen et al. [4] found that near the threshold  $\beta = \alpha$ . Thus one expects that close to  $p_c$ ,  $\beta = 1.3 = 1.33 = 0.97$  and the nonlinearity exponent for I-V characteristic is thus  $\beta = \alpha + 1 = 1.97$  in 2D. It will be noted that close to  $p_c$ , the nonlinearity exponent for our model in 2D is very close to it. Further, since the exponent  $\beta$  lies between about 3 and 1 for  $p$  between 0.3

and 0.9, the crossover exponent in our model can vary between 1.3 and 2 in the same dilution range in 2D.

Apart from calculating the nonlinearity exponent as discussed previously, one may also measure or calculate the difference between the conductance ( $G$ ) in the two asymptotic linear regimes. The two limiting conductances  $G_0$  and  $G_f$  are already defined in two asymptotic linear regimes namely,  $V \rightarrow 0$  and  $V \rightarrow 1$  respectively. Whereas the nonlinearity exponent ( $\alpha$  or  $\beta$ ) acts as a measure of the initial nonlinearity near the threshold  $V_g$ , the difference in conductance  $G_d = G_f - G_0$  serves as a measure of the overall nonlinearity. We have the following criteria which may be easily checked.

In the range  $p < p_c$ :  $G_0 = 0$  and  $G_f = 0$ , so  $G_d = 0$ ,

In the range  $p_c < p < p_1$ :  $G_0 = 0$  and  $G_f \neq 0$ , so  $G_d = G_f$ ,

In the range  $p < p < 1$ :  $G_0 > 0$  and  $G_d = G_f - G_0$ .

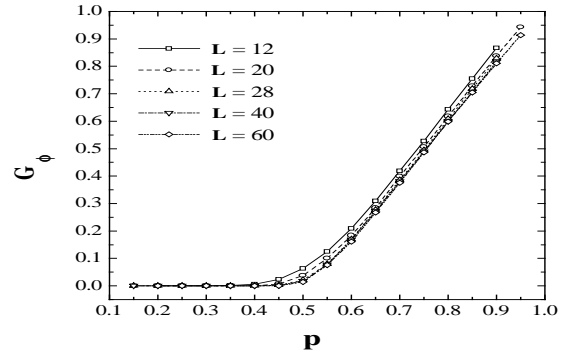


FIG. 12. The behavior of  $G_0$  against  $p$ . The system sizes ( $L$ ) are indicated in the figure.

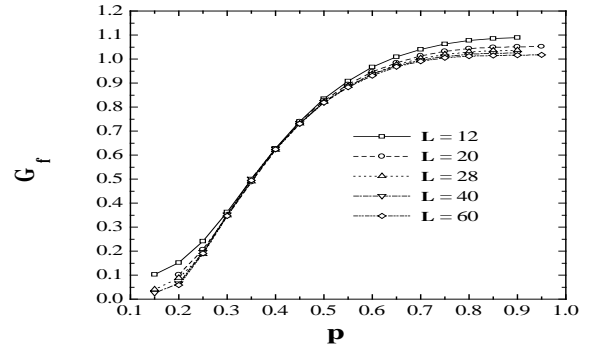


FIG. 13. The behavior of  $G_f$  against  $p$ . The system sizes ( $L$ ) are indicated in the figure.

We have shown the variation of  $G_0$  and  $G_f$  against  $p$  in Fig. 12 and in Fig. 13 respectively for a square network of size  $L = 12, 20, 28, 40$  and  $60$ . The averages are done over 100 to 1000 configurations in each case. The interesting point to note is that as a function of  $p$ ,  $G_f$  tends to be  $(p$ -independent) as  $p \rightarrow 1$  but  $G_0$  seems to be increasing sharply. Further, one may note that while  $G_0$  behaves in a power-law fashion around  $p_c = 0.5$ ,  $G_f$  does the same around  $p_{ct} = 0.181$ . Next, the difference in conductance  $G_d$  is plotted against  $p$  in Fig. 14. The peak in this curve appears at around  $p = p_c$ . This indicates that the overall nonlinearity is maximum near the geometrical percolation threshold. There does not seem to be any strong finite-size effects in the  $G_d$ - $p$  graph except close to  $p_{ct}$ .

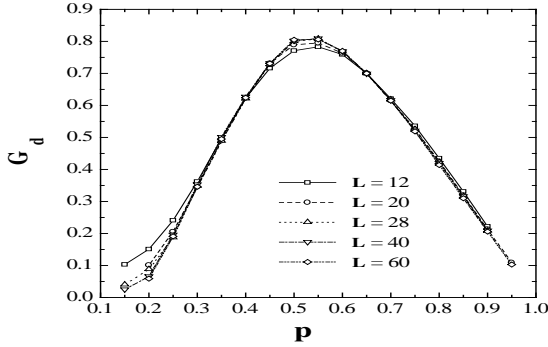


FIG. 14. The behavior of  $G_d$  against  $p$  for different system sizes  $L$  as indicated in the figure.

The next important question is how the difference in conductance  $G_d$  is related to the initial conductance  $G_0$ . The variation of  $G_d$  against  $G_0$  is shown in the Fig. 15 for the whole range of  $p$  (0 to 1). As expected, the peak appears at around  $p = p_{ct}$ , and a strong finite size effect may be noted in the  $G_d$ - $G_0$  graph. One may also observe that in the thermodynamic limit,  $G_d = 0$  for  $p \rightarrow p_{ct}$ . Now we would like to examine the above relationship, i.e.,  $G_d$  against  $G_0$  in the interval  $p_{ct} < p < 1$ . We do fit the data with the function  $G_d = A - B G_0^\gamma(L)$ , where  $A$  and  $B$  are constants and the exponent  $\gamma(L) > 0$ . The data were fitted for different system sizes from  $L = 8$  to  $80$ . In the Fig. 16 we have shown  $\gamma(L)$  against  $L$  to show the finite size behavior and find that  $\gamma(1) \approx 1.1$  which is close to 1. Thus we may conclude that  $G_d$  is almost linearly dependent on  $G_0$  in the limit of  $L \rightarrow 1$  which means that  $G_f$  is also linearly dependent on  $G_0$ . This in turn supports the idea of identical scaling relationship for two saturation conductances  $G_0$  and  $G_f$  around the respective thresholds ( $p_c$  and  $p_{ct}$ ). This is consistent with the fact that the system is in the same universality class in both the limits (i.e.,  $G_f \sim (p - p_{ct})^\tau$ ).

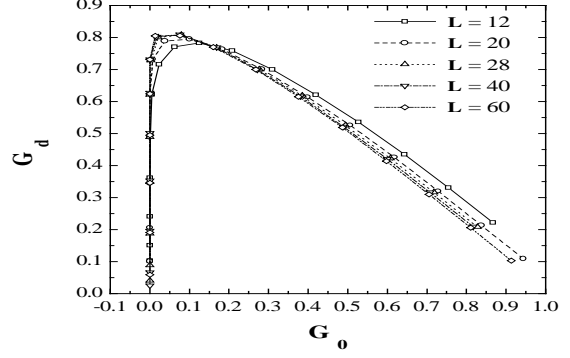


FIG. 15. The  $G_d$  against  $G_0$  for different  $L$  as indicated in the figure.

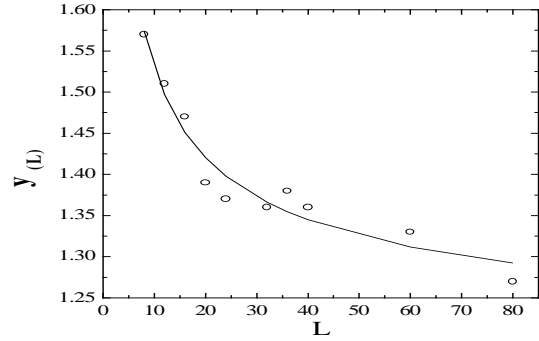


FIG. 16. The finite size behavior of  $\gamma(L)$ , for different  $L$  data fitted with  $\gamma(L) = \gamma(1) + B/L^r$  where  $\gamma(1) = 1.1$ ,  $B = 12$ ,  $r = 0.5$

#### C. Comparison with some EMA results

For the sake of comparison we plot the  $G_d$  against  $p$  and  $G_d$  against  $G_0$  curves with the corresponding results obtained by EMA for our model (in 2D). In Fig. 17 the  $G_d$  against  $p$  is plotted for both the simulation result and the EMA result. Both are shown for our model network in 2D, where the simulation result plotted is for  $L = 60$ . In Fig. 18 we plot  $G_d$  against  $G_0$  again for the simulation and the EMA result. It is apparent from the above two figures that these results are close.

The effective conductance of the network  $G_e = G_0$  when all the tunneling bonds behave as perfect insulators (the usual limit of binary mixture of conductors and insulators,  $p_c = 1/2$ ) and the effective conductance  $G_e = G_f$  when all the tunneling bonds (or resistors) behave as the ohmic conductors (Eq. (3.10)). Clearly, if one puts  $P_t = 0$  in Eq. (3.10), one finds that

$$G_0 = \frac{dP_0}{(d-1)}; \quad (4.11)$$

The behavior of  $G_d$  against  $p$  is shown in Fig. 17 for 2D.  $G_d$  has a maximum at  $p_c$  ( $= 1/2$  in 2D) as it should be because the system with the  $o$ -bonds only is most tenuous at the geometrical percolation threshold and the measure of nonlinearity clearly should be maximum there (with the largest concentration of the  $t$ -bonds). The plot of  $G_d$  against  $G_0$  is also shown in Fig. 18. In the same plot we have also shown the simulation result for comparison and one may note that the quantity  $G_d$  is maximum at  $p = p_c$ . The EMA result is quite close to the simulation result and the match becomes better as one goes farther and farther away from  $p_{ct}$ .

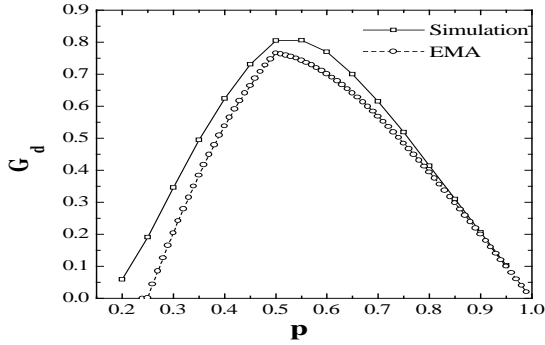


FIG. 17. The variation of  $G_d$  against  $p$ , obtained by the simulation and the EMA, are plotted for comparison.

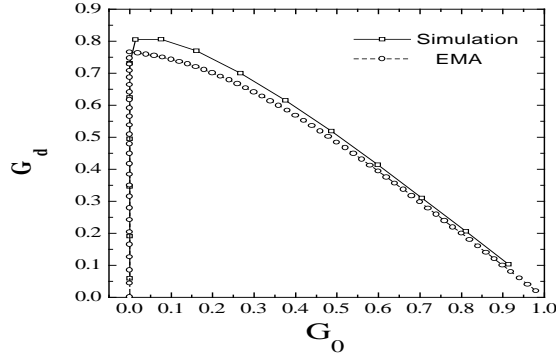


FIG. 18. The variation of  $G_d$  against  $G_0$ , obtained by the simulation and the EMA, are plotted for comparison.

## V. SUMMARY AND COMMENTS

In this paper, we have been mainly concerned with the nonlinear response characteristics, the relevant scaling

and related exponents in composites or granular metallic systems where transport due to charge tunneling plays an important role. One may note that our correlated percolation model and the corresponding RRTN network can capture the essential features related to nonlinearity quite well. Before ending we would like to make some comments and discussions for the sake of completeness. The existence of a well-defined voltage threshold ( $V_g$ ) close to which a power-law regime appears indicates that this threshold (breakdown) voltage is a critical point. Similar threshold behavior has been observed in pinned charge-density-wave (CDW) conductors, superconductors with pinned vortices (type-II), etc. Indeed it has been argued long ago that wherever there exists some sort of threshold of force for motion to occur, the threshold actually corresponds to a dynamic critical point [25] for the driven dynamical system. Disorder in such systems is known to give rise to 'pinning' or inhibition to transport upto a critical value of the force. Clearly in our percolation model, the threshold  $V_g$  acts as a dynamical critical point for the systems with volume fractions in the range  $p_{ct} < p < p_c$ . For such systems the field corresponding to the threshold voltage  $V_g$  is called the dielectric breakdown field and is pretty well-studied in the DRRN [16] type models. We have focussed on the threshold as a dynamical critical point in our discrete model, and calculated the breakdown exponent for our RRTN model elsewhere [26].

As we pointed out above (see also Ref. [14]) that the mechanism of nonlinearity is essentially the same both below and above the system threshold. Below the system threshold, there is no system spanning cluster. So the transport is identified as intercluster tunneling or hopping across dangling bonds or gaps. Above the threshold there are both intercluster and intracluster tunneling. But intracluster tunneling mechanism certainly dominates. The nearest neighbor gaps are everywhere; both inside the smaller isolated clusters as well as in the system spanning cluster. So the tunneling mechanism is operative both below and above  $p_c$  (in the interval  $p_{ct} < p < 1$ ) giving rise to nonlinear regime in the response.

From our analysis of current-voltage ( $I$ - $V$ ) data we understand that one does not do justice by fitting only the  $I$ - $V$  curve and finding out the nonlinearity exponent therefrom since that fitting is not robust. One may easily get tempted to fit the nonlinear regime of a  $I$ - $V$  curve in general through an  $n$ -th degree polynomial function. A reasonable choice [6] would be to fit with the law:  $I = G_1 V + G_2 V^3$ , assuming that the leading nonlinear term is cubic (ignoring other higher order terms). Even ignoring the fact that the nonlinearity exponent away from  $p_c$  are significantly different from integer values, we note that this type of analysis in this form may lead to confusion. The determination of the exponents and the coefficients may become arbitrary. Arbitrary selection of the range of  $I$ - $V$  data for this purpose and the fitting of that would account for this arbitrariness. One may not know upto what voltage scale (in the nonlin-

ear regime) one should fit the data and hence one may get a set of different answers for the values of the exponents. A typical I-V curve, for the kind of systems we address, can in general be fitted by a simple power-law:  $I \propto (V - V_g)^\alpha$ , at least around the threshold voltage  $V_g$ . But this also may not provide unambiguous answer most of the time. One may note that the exponent for such power-law does change continuously as the applied voltage  $V$  is increased from  $V_g$  and the I-V curve may ultimately approach another linear regime. In fact, the selection of the range of data and its fitting had been at the root of many confusing results as found in the literature. Instead our prescription of fitting of the G-V data for the entire nonlinear regime along with the saturation, as presented, is found to be most satisfactory. From such a fitting (Eq. (4.7)) of the G-V data, one can obtain the desired power-law and find the exponent. The G-V curves for the type of composites we focus our attention on, may all be generically fitted by a function like  $G(V) = G_0 + G_d f(V)$ , where  $f(V)$  is a function that behaves as  $V$  for small  $V$ , where  $V = V - V_g$ .  $f(V) \rightarrow 0$  as  $V \rightarrow 0$  and  $f(V) \rightarrow 1$  as  $V \rightarrow 1$  (or an appropriately large value for a given finite system).

Next we point out a few observations on some recent experiments in the literature which are found to be not in full agreement with our simulation results. In a recent experiment on the carbon-wax mixture [27] it is claimed that the conductivity exponent ( $t$ ) to be different in the two extreme limits namely,  $V \rightarrow 0$  and  $V \rightarrow 1$ . More explicitly and in the perspective of the foregoing discussion,  $G_0 \propto p^t$  and  $G_f \propto p^0$ , where  $p = (p - p_c)$ . Note that the  $p$  for the scaling of  $G_f$  should have been  $(p - p_t)$  as we have discussed before. In any case, it is claimed that  $t^0 \neq t$ . More specially,  $t^0 = ct$ , where  $c = 0.76$  (in 3D) as reported [27]. This in turn is related to the question of universality class, claiming that the system goes over to different universality class in the saturation limit ( $V \rightarrow 1$ ) (has been termed as altered percolating state in Ref. [27]). However, as we discuss in section IV B (we have also claimed earlier [18]) that the system seems to be in the same universality class in both the limits whereby we claim that  $t = t^0$  within the numerical accuracy. Our calculation of course is in 2D. But the essential physics should remain the same as we go over to 3D.

We have seen that the nonlinearity exponent,  $(\alpha + 1)$  varies significantly with the volume fraction ( $p$ ) of the conducting component, the minimum value of the exponent being around 2.0 at  $p = p_c$ . Chen and Johnson, in their experiment on Ag-KCl [7], found the above nonlinearity exponent to vary with  $p$ . In particular they found that for a sample very close to percolation threshold, the nonlinearity exponent is as large as 20. In another early and a very prominent experiment, nonlinear response in ZnO varistors has been addressed by Mahan et al. [29]. The observed I-V characteristics in the ZnO varistors are often empirically described by the power-law relation:

$$I = kV^\alpha; \quad (5.1)$$

where the parameter ( $\alpha > 1$ ) is the measure of nonlinearity. A theory had been developed by Mahan et al. to predict the coefficient of nonlinearity ( $\alpha$ ) as high as 50 or even 100. Such a high value of  $\alpha$  of course indicates an exponential relationship rather than a power-law. Canessa and Nguyen [30] had attempted a computer simulation study of the varistors considering a binary mixture model to understand the very high value of  $\alpha$ .

Intrigued by these results we ran some test for a square lattice with ( $L=20$  and  $40$ )  $p=0.2$ , very close to our  $p_{ct}$ . We obtained in our preliminary analysis by fitting  $G$  with voltage  $V$  that  $\alpha > 20$  for  $L=20$  and  $\alpha \rightarrow 1$  (diverging for ever) for  $L=40$ . This was very suspicious and by zooming into the fitting close to the threshold ( $V_g$ ), we found the fitting to be extremely bad. The other functions listed before (including the double-exponential) did not give any better fitting either. But this is the region which gives the initial power-law exponent. To get the  $t$  better in this region, we fitted the logarithmic conductance ( $\ln G$ ), keeping our fitting function the same Eq. (4.7) as before. Then we found the exponent to be of the order of 3 (the Fig. 11 was done by taking care of this fitting problem). Thus power-law description still seems to hold but there seems to be a different problem close to  $p_{ct}$ . Since the fitting was still not as good as at higher  $p > 0.4$ , we wanted to check if the averaging process itself is at flaw at very low volume fractions. Hence we look at the distribution of the current ( $I$ ) for different realizations of the sample of size  $L=20$  and  $p=0.2$  for two different voltages. In Fig.19, the histogram is shown for  $V=5$ , and in Fig.20, the same is shown for  $V=10$ . The distribution for  $V=10$  is reasonably well behaved, but the one for  $V=5$  has an isolated delta-function-like peak at zero conductance apart from two other broader peaks at higher conductances. We did also look at the relative value of the variance (relative to the mean squared) defined as

$$RV = \frac{(\langle I^2 \rangle - \langle I \rangle^2)}{\langle I \rangle^2} \quad (5.2)$$

If this value is less than 1, averaging is alright, but if it is much larger than 1, the self-averaging property of the distribution does not work. We have tested that  $RV$  is about 3.3 for the set of data for  $V=5$  and it is about 0.3 for  $V=10$ . Thus the low  $p$  samples are non-self-averaging at low voltages but tend to be more self-averaging at higher voltages. This property was also reported for quantum systems by Lenstra and Smokers [31], and thus our semi-classical model of percolation indeed seems to capture some non-classical (quantum) behavior at low  $p$  as expected.

The connection between the above exponent and the crossover exponent ( $\alpha$ ) is the following. The crossover voltage  $V_c$  is related to the initial nonzero conductance  $G_0$  by  $V_c = G_0^{\alpha-1}$ . But from Eq. (4.10) we know that the excess conductance  $G(V) = V$  for small  $V$ .

Choosing  $G = G_0$  for an arbitrary but small and if one is close to percolation threshold, one has  $V_c = G_0^{-1}$  which implies that  $\beta = 1/(x - 1)$ . Thus, as the value of nonlinearity exponent is dependent on  $p$ , the crossover exponent ( $x$ ) should also be dependent on  $p$ . The values of the crossover exponent  $x$  so far reported in the literature are for the experimental data for the samples close to but above the threshold. But we may conclude that this exponent should also show change with  $p$  if  $p$  is away from  $p_c$ . In fact, such an example may be mentioned here. The crossover exponent is found to be widely different for a set of samples as measured recently [28]. The reason for this is yet to be understood. But if the samples taken for measurements have widely different volume fractions ( $p$ ) of conducting components, then nonlinearity exponent and thus the crossover exponent for them could be widely different.

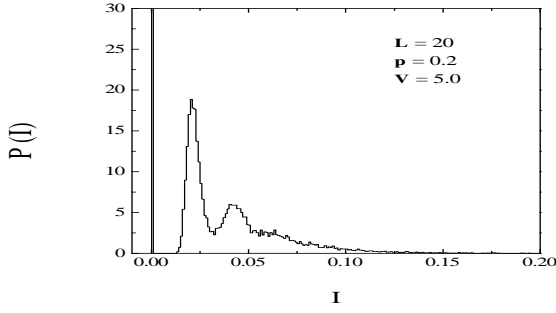


FIG. 19. The distribution of current ( $I$ ) in the 2D square network of size  $L = 20$  for  $p = 0.2$  and an applied voltage  $V = 5.0$ . This distribution is non-self-averaging.  $6 \times 10^4$  configurations were used for this purpose.

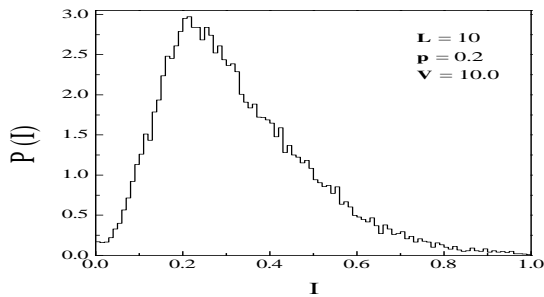


FIG. 20. The distribution of current ( $I$ ) in the 2D square network of size  $L = 10$  for  $p = 0.2$  and an applied voltage  $V = 10.0$ . This distribution is self-averaging.  $2 \times 10^4$  configurations were used for this purpose.

Now it may be noted that if  $\beta > 1$  or in other words  $\beta > 1$  in the Eq. (4.7), the first derivative of  $G$  with respect to  $V$ , i.e.,  $dG/dV$  would attain a maximum value at the inflexion point (at some voltage in the nonlinear regime). We fitted a set of  $G-V$  and the corresponding  $dG/dV-V$  data (see Ref. [24]), taken from the experimental observations on a carbon-wax composite system [5] to show the appearance of a peak in the  $dG/dV-V$  curve. To indicate how good or bad our fitting equation is, we fit the above data set for  $G-V$  characteristics by the Eq. (4.7). The fitted line is seen to match the experimental data very well with the above function. As a further test of the fitting, we took the parameters of the  $G-V$  fit, and used them (the functional form) to obtain  $dG/dV$  as a function of  $V$ . The agreement with the experimental values for  $dG/dV$  should be considered rather good given that  $G$  and  $dG/dV$  are independent measurements and that higher the harmonic more error-prone is its value. Incidentally, the nonlinearity exponent for this 3D experimental data fitted by our method comes out to be 1.74, where the crossover exponent measurement on the same sample would give an  $\beta$ -value of about 2.

#### V I. ACKNOWLEDGEMENT

We thank K.K. Bardhan, R.K. Chakrabarty and U. Nandy for allowing us to go through their experimental data and for the related discussions. We are also thankful to B.K. Chakrabarti, S. Roux and H.J. Hermann for many useful discussions.

- 
- [1] For quite high voltages, other more complicated situations (e.g., negative differential conductance) may arise, but we do not address them in our work discussed here.
  - [2] Even in this semi-classical sense, these barriers are still fundamentally different from the Ohmic resistors since they contribute to the resistance but not to heat dissipation.
  - [3] L. de Arcangelis, S. Redner and H.J. Hermann, J. Physique Lett. 46, L-585 (1985)
  - [4] L.K.H. van Beek and B.J.C.F. van Pul, Carbon 2, 121 (1964); G.E. Pike and C.H. Seager, J. Appl. Phys. 48, 5152 (1977); E.K. Sichel, J.L. Gittleman and P. Sheng, Phys. Rev. B 18, 5712 (1978); D. van der Putten, J.T. Moomen, H.B. Brom, J.C.M. Brokken-Zijp and M.A.J. Michels, Phys. Rev. Lett. 69, 494 (1992); Y. Gefen, W.-H. Shih, R.B. Laibowitz and J.M. Viggiano, Phys. Rev. Lett. 57, 3097 (1986); M. Prester, E. Babic, M. Stubicar and P. Nozar, Phys. Rev. B 49, 6967 (1994)
  - [5] (a) K.K. Bardhan and R.K. Chakrabarty, Phys. Rev. Lett. 69, 2559 (1992); (b) Phys. Rev. Lett. 72, 1068 (1994)

- [6] R.K. Chakrabarty, K.K. Bardhan and A. Basu, J. Phys.: Condens. Matter, 5, 2377 (1993); see also J. Robertson, Amorphous Carbon, Adv. Phys. 35, 318-374 (1986) for lamellated structure of a-C.
- [7] I-G. Chen and W.B. Johnson, J. Mat. Sc. 27, 5497 (1992)
- [8] I. Balberg, Phys. Rev. Lett., 59, 1305 (1987)
- [9] P. Mandal, A. Neumann, A.G.M. Jansen, P. Wyder and R. Delbour, Phys. Rev. B, 55, 452 (1997)
- [10] Reghu M., C.O. Yoon, C.Y. Yang, D. Moses, P. Smith and A.J. Heeger, Phys. Rev. B, 50, 13931 (1994)
- [11] A.J. Rimberg, T.R. Ho and J. Clarke, Phys. Rev. Lett. 74, 4714 (1995)
- [12] A.A. Middleton and N.S. Wingreen, Phys. Rev. Lett. 71, 3198 (1993)
- [13] M. Aertsens and J. Naudts in Phase Transitions in Soft Condensed Matter eds. T. Riste and D. Sherrington, NATO ASI Series B: Phys. Vol. 211
- [14] A.K. Sen and A.K. Gupta in Non-linearity and Breakdown in Soft Condensed Matter, eds. K.K. Bardhan, B.K. Chakrabarti and A. Hansen, Lecture Notes in Physics, 437, 271 (Springer-Verlag, Berlin 1994)
- [15] M. Sahini in Annual Reviews of Computational Physics II, pp. 175, eds. D. Stauffer (World Scientific, 1995)
- [16] There exists a similar model in the literature called a dynamic random resistor network (DRRN) as applied by Gefen et al. [4] to explain the crossover exponent in the experiment on Au-In reported in the same reference. The difference between these two models lies in the fact that the tunneling elements (or the imperfect insulators) in the DRRN could be anywhere in the non-metallic domain of the system whereas in the RRTN, these elements exist only in the proximity gap between two metallic domains (one can imagine that the charge transfer by tunneling should be most effective only in such gaps). It may also be noted that traditionally the dielectric breakdown problem has been treated in the DRRN type models.
- [17] It may be noted that if we include tunneling between next nearest neighbors also, the effective percolation threshold would go down even further. For simplicity, in this work we restrict ourselves to nearest neighbor tunneling only.
- [18] A.K. Gupta and A.K. Sen, Physica A, 215, 1-9 (1995)
- [19] D.G. Buggeman, Ann. Phys. (Leipz.) 24, 636 (1935)
- [20] R. Landauer, J. Appl. Phys. 23, 779 (1952)
- [21] S. Kirkpatrick, Rev. Mod. Phys. 45, 574 (1973)
- [22] P.M. Hui in Non-linearity and Breakdown in Soft Condensed Matter, eds. K.K. Bardhan, B.K. Chakrabarti and A. Hansen, Lecture Notes in Physics, 437, 271 (Springer-Verlag, Berlin 1994)
- [23] S. Roux and H.J. Hermann, Europhys. Lett. 4, 1227 (1987)
- [24] A.K. Gupta, Ph.D. thesis, Jadavpur University (submitted)
- [25] S.A. Wolf, D.J. Gubser, and Y. Imry, Phys. Rev. Lett., 42, 324 (1979); D.S. Fisher, Phys. Rev. Lett., 68, 670 (1983); A.A. Middleton and N.S. Wingreen, Phys. Rev. Lett., 71, 3198 (1993)
- [26] A.K. Gupta and A.K. Sen, Physica A, in press (1997)
- [27] U.N. Nandy and K.K. Bardhan, Europhys. Lett. 31, 101 (1995)
- [28] U.N. Nandy and K.K. Bardhan (private communication)
- [29] G.D. Mahan, Lionel M. Levinson, and H.R. Philipp, J. Appl. Phys. 50, 2799 (1979)
- [30] E. Canessa and V.L. Nguyen, Physica B 179, 335 (1992)
- [31] D. Lenstra and R.T.M. Smokers, Phys. Rev. B 38, 6452 (1988)